

Color Coherent Radiation in Multijet Events from $p\bar{p}$ Collisions at $\sqrt{s} = 1.8$ TeV

B. Abbott,²⁹ M. Abolins,²⁶ B.S. Acharya,⁴⁴ I. Adam,¹² D.L. Adams,³⁸ M. Adams,¹⁷ S. Ahn,¹⁴ H. Aihara,²² G.A. Alves,¹⁰ E. Amidi,³⁰ N. Amos,²⁵ E.W. Anderson,¹⁹ R. Astur,⁴³ M.M. Baarmand,⁴³ A. Baden,²⁴ V. Balamurali,³³ J. Balderston,¹⁶ B. Baldin,¹⁴ S. Banerjee,⁴⁴ J. Bantly,⁵ J.F. Bartlett,¹⁴ K. Bazizi,⁴⁰ A. Belyaev,²⁷ S.B. Beri,³⁵ I. Bertram,³² V.A. Bezzubov,³⁶ P.C. Bhat,¹⁴ V. Bhatnagar,³⁵ M. Bhattacharjee,¹³ N. Biswas,³³ G. Blazey,³¹ S. Blessing,¹⁵ P. Bloom,⁷ A. Boehnlein,¹⁴ N.I. Bojko,³⁶ F. Borchering,¹⁴ C. Boswell,⁹ A. Brandt,¹⁴ R. Brock,²⁶ A. Bross,¹⁴ D. Buchholz,³² V.S. Burtovoi,³⁶ J.M. Butler,³ W. Carvalho,¹⁰ D. Casey,⁴⁰ Z. Casilum,⁴³ H. Castilla-Valdez,¹¹ D. Chakraborty,⁴³ S.-M. Chang,³⁰ S.V. Chekulaev,³⁶ L.-P. Chen,²² W. Chen,⁴³ S. Choi,⁴² S. Chopra,²⁵ B.C. Choudhary,⁹ J.H. Christenson,¹⁴ M. Chung,¹⁷ D. Claes,²⁸ A.R. Clark,²² W.G. Cobau,²⁴ J. Cochran,⁹ W.E. Cooper,¹⁴ C. Cretsinger,⁴⁰ D. Cullen-Vidal,⁵ M.A.C. Cummings,¹⁶ D. Cutts,⁵ O.I. Dahl,²² K. Davis,² K. De,⁴⁵ K. Del Signore,²⁵ M. Demarteau,¹⁴ D. Denisov,¹⁴ S.P. Denisov,³⁶ H.T. Diehl,¹⁴ M. Diesburg,¹⁴ G. Di Loreto,²⁶ P. Draper,⁴⁵ Y. Ducros,⁴¹ L.V. Dudko,²⁷ S.R. Dugad,⁴⁴ D. Edmunds,²⁶ J. Ellison,⁹ V.D. Elvira,⁴³ R. Engelmann,⁴³ S. Eno,²⁴ G. Eppley,³⁸ P. Ermolov,²⁷ O.V. Eroshin,³⁶ V.N. Evdokimov,³⁶ T. Fahland,⁸ M. Fatyga,⁴ M.K. Fatyga,⁴⁰ S. Feher,¹⁴ D. Fein,² T. Ferbel,⁴⁰ G. Finocchiaro,⁴³ H.E. Fisk,¹⁴ Y. Fisyaik,⁷ E. Flattum,¹⁴ G.E. Forden,² M. Fortner,³¹ K.C. Frame,²⁶ S. Fuess,¹⁴ E. Gallas,⁴⁵ A.N. Galyaev,³⁶ P. Garton,⁹ T.L. Geld,²⁶ R.J. Genik II,²⁶ K. Genser,¹⁴ C.E. Gerber,¹⁴ B. Gibbard,⁴ S. Glenn,⁷ B. Gobbi,³² M. Goforth,¹⁵ A. Goldschmidt,²² B. Gómez,¹ G. Gómez,²⁴ P.I. Goncharov,³⁶ J.L. González Solís,¹¹ H. Gordon,⁴ L.T. Goss,⁴⁶ K. Gounder,⁹ A. Goussiou,⁴³ N. Graf,⁴ P.D. Grannis,⁴³ D.R. Green,¹⁴ J. Green,³¹ H. Greenlee,¹⁴ G. Grim,⁷ S. Grinstein,⁶ N. Grossman,¹⁴ P. Grudberg,²² S. Grünendahl,⁴⁰ G. Guglielmo,³⁴ J.A. Guida,² J.M. Guida,⁵ A. Gupta,⁴⁴ S.N. Gurzhiev,³⁶ P. Gutierrez,³⁴ Y.E. Gutnikov,³⁶ N.J. Hadley,²⁴ H. Haggerty,¹⁴ S. Hagopian,¹⁵ V. Hagopian,¹⁵ K.S. Hahn,⁴⁰ R.E. Hall,⁸ P. Hanlet,³⁰ S. Hansen,¹⁴ J.M. Hauptman,¹⁹ D. Hedin,³¹ A.P. Heinson,⁹ U. Heintz,¹⁴ R. Hernández-Montoya,¹¹ T. Heuring,¹⁵ R. Hirosky,¹⁵ J.D. Hobbs,¹⁴ B. Hoeneisen,^{1,*} J.S. Hoftun,⁵ F. Hsieh,²⁵ Ting Hu,⁴³ Tong Hu,¹⁸ T. Huehn,⁹ A.S. Ito,¹⁴ E. James,² J. Jaques,³³ S.A. Jerger,²⁶ R. Jesik,¹⁸ J.Z.-Y. Jiang,⁴³ T. Joffe-Minor,³² K. Johns,² M. Johnson,¹⁴ A. Jonckheere,¹⁴ M. Jones,¹⁶ H. Jöstlein,¹⁴ S.Y. Jun,³² C.K. Jung,⁴³ S. Kahn,⁴ G. Kalbfleisch,³⁴ J.S. Kang,²⁰ D. Karmgard,¹⁵ R. Kehoe,³³ M.L. Kelly,³³ C.L. Kim,²⁰ S.K. Kim,⁴² A. Klatchko,¹⁵ B. Klima,¹⁴ C. Klopfenstein,⁷ V.I. Klyukhin,³⁶ V.I. Kochetkov,³⁶ J.M. Kohli,³⁵ D. Koltick,³⁷ A.V. Kostritskiy,³⁶ J. Kotcher,⁴ A.V. Kotwal,¹² J. Kourlas,²⁹ A.V. Kozelov,³⁶ E.A. Kozlovski,³⁶ J. Krane,²⁸ M.R. Krishnaswamy,⁴⁴ S. Krzywdzinski,¹⁴ S. Kunori,²⁴ S. Lami,⁴³ H. Lan,^{14,†} R. Lander,⁷ F. Landry,²⁶ G. Landsberg,¹⁴ B. Lauer,¹⁹ A. Leflat,²⁷ H. Li,⁴³ J. Li,⁴⁵ Q.Z. Li-Demarteau,¹⁴ J.G.R. Lima,³⁹ D. Lincoln,²⁵ S.L. Linn,¹⁵ J. Linnemann,²⁶ R. Lipton,¹⁴ Y.C. Liu,³² F. Lobkowicz,⁴⁰ S.C. Loken,²² S. Lökös,⁴³ L. Lueking,¹⁴ A.L. Lyon,²⁴ A.K.A. Maciel,¹⁰ R.J. Madaras,²² R. Madden,¹⁵ L. Magaña-Mendoza,¹¹ S. Mani,⁷ H.S. Mao,^{14,†} R. Markeloff,³¹ T. Marshall,¹⁸ M.I. Martin,¹⁴ K.M. Mauritz,¹⁹ B. May,³² A.A. Mayorov,³⁶ R. McCarthy,⁴³ J. McDonald,¹⁵ T. McKibben,¹⁷ J. McKinley,²⁶ T. McMahon,³⁴

H.L. Melanson,¹⁴ M. Merkin,²⁷ K.W. Merritt,¹⁴ H. Miettinen,³⁸ A. Mincer,²⁹
 C.S. Mishra,¹⁴ N. Mokhov,¹⁴ N.K. Mondal,⁴⁴ H.E. Montgomery,¹⁴ P. Mooney,¹
 H. da Motta,¹⁰ C. Murphy,¹⁷ F. Nang,² M. Narain,¹⁴ V.S. Narasimham,⁴⁴ A. Narayanan,²
 H.A. Neal,²⁵ J.P. Negret,¹ P. Nemethy,²⁹ M. Nicola,¹⁰ D. Norman,⁴⁶ L. Oesch,²⁵
 V. Oguri,³⁹ E. Oltman,²² N. Oshima,¹⁴ D. Owen,²⁶ P. Padley,³⁸ M. Pang,¹⁹ A. Para,¹⁴
 Y.M. Park,²¹ R. Partridge,⁵ N. Parua,⁴⁴ M. Paterno,⁴⁰ J. Perkins,⁴⁵ M. Peters,¹⁶
 R. Piegai,⁶ H. Piekarz,¹⁵ Y. Pischalnikov,³⁷ V.M. Podstavkov,³⁶ B.G. Pope,²⁶
 H.B. Prosper,¹⁵ S. Protopopescu,⁴ J. Qian,²⁵ P.Z. Quintas,¹⁴ R. Raja,¹⁴ S. Rajagopalan,⁴
 O. Ramirez,¹⁷ L. Rasmussen,⁴³ S. Reucroft,³⁰ M. Rijssenbeek,⁴³ T. Rockwell,²⁶ N.A. Roe,²²
 P. Rubinov,³² R. Ruchti,³³ J. Rutherford,² A. Sánchez-Hernández,¹¹ A. Santoro,¹⁰
 L. Sawyer,²³ R.D. Schamberger,⁴³ H. Schellman,³² J. Sculli,²⁹ E. Shabalina,²⁷ C. Shaffer,¹⁵
 H.C. Shankar,⁴⁴ R.K. Shivpuri,¹³ M. Shupe,² H. Singh,⁹ J.B. Singh,³⁵ V. Sirotenko,³¹
 W. Smart,¹⁴ R.P. Smith,¹⁴ R. Snihur,³² G.R. Snow,²⁸ J. Snow,³⁴ S. Snyder,⁴ J. Solomon,¹⁷
 P.M. Sood,³⁵ M. Sosebee,⁴⁵ N. Sotnikova,²⁷ M. Souza,¹⁰ A.L. Spadafora,²²
 R.W. Stephens,⁴⁵ M.L. Stevenson,²² D. Stewart,²⁵ F. Stichelbaut,⁴³ D.A. Stoianova,³⁶
 D. Stoker,⁸ M. Strauss,³⁴ K. Streets,²⁹ M. Strovink,²² A. Sznajder,¹⁰ P. Tamburello,²⁴
 J. Tarazi,⁸ M. Tartaglia,¹⁴ T.L.T. Thomas,³² J. Thompson,²⁴ T.G. Trippe,²² P.M. Tuts,¹²
 N. Varelas,²⁶ E.W. Varnes,²² D. Vititoe,² A.A. Volkov,³⁶ A.P. Vorobiev,³⁶ H.D. Wahl,¹⁵
 G. Wang,¹⁵ J. Warchol,³³ G. Watts,⁵ M. Wayne,³³ H. Weerts,²⁶ A. White,⁴⁵ J.T. White,⁴⁶
 J.A. Wightman,¹⁹ S. Willis,³¹ S.J. Wimpenny,⁹ J.V.D. Wirjawan,⁴⁶ J. Womersley,¹⁴
 E. Won,⁴⁰ D.R. Wood,³⁰ H. Xu,⁵ R. Yamada,¹⁴ P. Yamin,⁴ J. Yang,²⁹ T. Yasuda,³⁰
 P. Yepes,³⁸ C. Yoshikawa,¹⁶ S. Youssef,¹⁵ J. Yu,¹⁴ Y. Yu,⁴² Z.H. Zhu,⁴⁰ D. Zieminska,¹⁸
 A. Zieminski,¹⁸ E.G. Zverev,²⁷ and A. Zylberstejn⁴¹

(DØ Collaboration)

¹*Universidad de los Andes, Bogotá, Colombia*

²*University of Arizona, Tucson, Arizona 85721*

³*Boston University, Boston, Massachusetts 02215*

⁴*Brookhaven National Laboratory, Upton, New York 11973*

⁵*Brown University, Providence, Rhode Island 02912*

⁶*Universidad de Buenos Aires, Buenos Aires, Argentina*

⁷*University of California, Davis, California 95616*

⁸*University of California, Irvine, California 92697*

⁹*University of California, Riverside, California 92521*

¹⁰*LAFEX, Centro Brasileiro de Pesquisas Físicas, Rio de Janeiro, Brazil*

¹¹*CINVESTAV, Mexico City, Mexico*

¹²*Columbia University, New York, New York 10027*

¹³*Delhi University, Delhi, India 110007*

¹⁴*Fermi National Accelerator Laboratory, Batavia, Illinois 60510*

¹⁵*Florida State University, Tallahassee, Florida 32306*

¹⁶*University of Hawaii, Honolulu, Hawaii 96822*

¹⁷*University of Illinois at Chicago, Chicago, Illinois 60607*

¹⁸*Indiana University, Bloomington, Indiana 47405*

¹⁹*Iowa State University, Ames, Iowa 50011*

- ²⁰*Korea University, Seoul, Korea*
- ²¹*Kyungsoong University, Pusan, Korea*
- ²²*Lawrence Berkeley National Laboratory and University of California, Berkeley, California 94720*
- ²³*Louisiana Tech University, Ruston, Louisiana 71272*
- ²⁴*University of Maryland, College Park, Maryland 20742*
- ²⁵*University of Michigan, Ann Arbor, Michigan 48109*
- ²⁶*Michigan State University, East Lansing, Michigan 48824*
- ²⁷*Moscow State University, Moscow, Russia*
- ²⁸*University of Nebraska, Lincoln, Nebraska 68588*
- ²⁹*New York University, New York, New York 10003*
- ³⁰*Northeastern University, Boston, Massachusetts 02115*
- ³¹*Northern Illinois University, DeKalb, Illinois 60115*
- ³²*Northwestern University, Evanston, Illinois 60208*
- ³³*University of Notre Dame, Notre Dame, Indiana 46556*
- ³⁴*University of Oklahoma, Norman, Oklahoma 73019*
- ³⁵*University of Panjab, Chandigarh 16-00-14, India*
- ³⁶*Institute for High Energy Physics, 142-284 Protvino, Russia*
- ³⁷*Purdue University, West Lafayette, Indiana 47907*
- ³⁸*Rice University, Houston, Texas 77005*
- ³⁹*Universidade do Estado do Rio de Janeiro, Brazil*
- ⁴⁰*University of Rochester, Rochester, New York 14627*
- ⁴¹*CEA, DAPNIA/Service de Physique des Particules, CE-SACLAY, Gif-sur-Yvette, France*
- ⁴²*Seoul National University, Seoul, Korea*
- ⁴³*State University of New York, Stony Brook, New York 11794*
- ⁴⁴*Tata Institute of Fundamental Research, Colaba, Mumbai 400005, India*
- ⁴⁵*University of Texas, Arlington, Texas 76019*
- ⁴⁶*Texas A&M University, College Station, Texas 77843*

(May 9, 2019)

Abstract

We report on a study of color coherence effects in $p\bar{p}$ collisions at a center of mass energy $\sqrt{s} = 1.8$ TeV. The data were collected with the DØ detector during the 1992–1993 run of the Fermilab Tevatron Collider. We observe the presence of initial–to–final state color interference with the spatial correlations between soft and hard jets in multijet events in the central and in forward pseudorapidity regions. The results are compared to Monte Carlo simulations with different color coherence implementations and to the predictions of $\mathcal{O}(\alpha_s^3)$ QCD calculations.

Color coherence phenomena in the final state have been very well established in e^+e^- annihilations [1–6], in what has been termed the “string” [7] or “drag” [8] effect. Particle production in the region between the quark and antiquark jets in $e^+e^- \rightarrow q\bar{q}g$ events is suppressed. In perturbative quantum chromodynamics (QCD) such effects arise from interference between the soft gluons radiated from the q , \bar{q} , and g . While quantum mechanical interference effects are expected in QCD, it is important to investigate whether such effects survive the nonperturbative hadronization process, for a variety of reactions over a broad kinematic range, as predicted by local parton–hadron duality [8].

The study of coherence effects in hadron–hadron collisions is considerably more subtle than that in e^+e^- annihilations due to the presence of colored constituents in both the initial and final states. The structure of multijet events in hard processes is influenced by the underlying color configurations at short distances. During a hard interaction, color is transferred from one parton to another and the color–connected partons act as color antennae. Examples of color flow diagrams are shown in Fig. 1 for $q\bar{q}$ and qg scattering. In Fig. 1a ($q\bar{q}$) the color system in which interference occurs is entirely between the initial and final states, whereas in Fig. 1b (qg) interference also occurs both in the initial and in final states due to their explicit color connection. Gluon radiation from the incoming and outgoing partons forms jets of hadrons around the direction of these colored emitters. The soft gluon radiation pattern accompanying any hard partonic system can be represented, to leading order in $1/N_c$ where N_c is the number of colors, as a sum of contributions corresponding to the color–connected partons. Within the perturbative calculations, this is a direct consequence of interferences between the radiation of various color emitters, resulting in the QCD coherence effects [8–10].

Color coherence, which results in a suppression of soft gluon radiation in the partonic cascade in certain regions of phase space, can be approximated by *Angular Ordering* (AO). For the case of outgoing partons, AO requires that the emission angles of soft gluons decrease monotonically as the partonic cascade evolves away from the hard process. The radiation is confined to a cone centered on the direction of one parton, and is bounded by the direction of its color–connected partner. Outside this region the interference of different emission diagrams becomes destructive and the azimuthally integrated amplitude vanishes to leading order. Conversely the emission angles increase for the incoming partons as the process develops from the initial hadrons to the hard subprocess. Monte Carlo simulations including coherence effects probabilistically by means of AO are available for both initial and final state evolutions. Conventional perturbative QCD calculations taken to sufficiently high order should in principle incorporate these effects to any accuracy. Use of the latter approach is limited, however, due to the current lack of such calculations beyond order α_s^3 .

Evidence for color coherence effects between initial and final states in $p\bar{p}$ interactions has been previously published [11] for the central pseudorapidity region. In this paper we report on a new study of initial–to–final state color coherence phenomena in $p\bar{p}$ interactions which also extends the measurements into the untested forward region. We compare our central and forward measurements to the predictions of $\mathcal{O}(\alpha_s^3)$ QCD matrix element calculations as well as to several parton–shower Monte Carlo (MC) simulations. This is the first direct comparison of such measurements to analytic $\mathcal{O}(\alpha_s^3)$ QCD predictions.

The DØ detector is described in detail elsewhere [12]. This analysis uses the uranium liquid–argon sampling calorimeter to measure jet final states. The DØ calorimeter has fine

segmentation in both azimuthal angle ϕ , and in pseudorapidity $\eta = -\ln[\tan(\theta/2)]$, where θ is the polar angle of the jet with respect to the proton beam. It has hermetic coverage for $|\eta| < 4$ with fractional transverse energy E_T resolution of $\sim 80\%/\sqrt{E_T(\text{GeV})}$ for jets.

The data sample for this analysis [13], representing an integrated luminosity of 8 pb^{-1} , was collected during the 1992–1993 Tevatron Collider run. Events were selected using a three level trigger. The first level required a coincidence of two scintillator hodoscopes located on either side of the interaction region, to ensure an inelastic collision. The next stage required the transverse energy of at least three calorimeter towers (0.2×0.2 in $\Delta\eta \times \Delta\phi$) to exceed a 7 GeV threshold in the region $|\eta| < 3.2$. The surviving events were analyzed by an online processor farm where jets were reconstructed using a simplified version of the final jet finding algorithm and an event was recorded to tape if it had a jet with $E_T > 85$ GeV.

Jets were reconstructed offline using an iterative fixed-cone clustering algorithm with cone radius $R = \sqrt{(\Delta\eta)^2 + (\Delta\phi)^2} = 0.5$. Spurious jets from isolated noisy calorimeter cells and accelerator losses were eliminated by loose cuts on the jet shape. The E_T of each jet was corrected for offsets due to the underlying event, multiple $p\bar{p}$ interactions, and noise; out-of-cone showering; and detector energy response as determined from the missing transverse energy balance of photon-jets events [14]. Events were required to have a measured vertex within 50 cm of the detector center.

The remaining events were required to have three or more reconstructed jets. Jets were ordered in E_T and labeled $E_{T1} > E_{T2} > E_{T3}$. We required $E_{T1} > 115$ GeV to avoid any bias introduced by the trigger threshold, and the third jet to have $E_T > 15$ GeV. Color coherence effects are measured with the angular distribution in (η, ϕ) space of the softer third jet around the second jet. The polar variables R and $\beta = \tan^{-1}(\frac{\text{sign}(\eta_2) \cdot \Delta\phi_{32}}{\Delta\eta_{32}})$ were used to locate the third jet in a search disk of $0.6 < R < \frac{\pi}{2}$ around the second jet (Fig. 2). Here, η_i and ϕ_i are the pseudorapidity and azimuthal angle of the i^{th} jet, $\Delta\eta_{32} = \eta_3 - \eta_2$, and $\Delta\phi_{32} = \phi_3 - \phi_2$. We define $\beta = 0$ to point towards the beam nearest to the second jet, and $\beta = \pi$ to point towards the farther beam. We study the interference effects in regions $|\eta_2| < 0.7$ and $0.7 < |\eta_2| < 1.5$. The pseudorapidity of the leading jet was not constrained, but the first and second jets were required to be in opposite ϕ hemispheres, i.e. $\frac{\pi}{2} < \Delta\phi_{21} < \frac{3\pi}{2}$. After all selection criteria, a sample of 9,048 (5,776) events remains in the central (forward) region.

The measured angular distributions (Fig. 3) are compared to the predictions of several MC simulations that differ in their implementation of color coherence. We employ the parton-shower MC event generators ISAJET 7.13 [15], HERWIG 5.8 [16], and PYTHIA 5.7 [17], and a partonic event generator, JETRAD 1.2 [18] to calculate the $\mathcal{O}(\alpha_s^3)$ QCD predictions. The ISAJET generator uses an independent shower development model without any color coherence effects. Both HERWIG and PYTHIA incorporate initial and final state color interference effects by means of the AO approximation of the parton cascades. In PYTHIA, the AO constraint can be turned off. HERWIG and PYTHIA each employ a phenomenological model to describe the hadronization process. HERWIG uses the cluster hadronization model and PYTHIA implements the Lund string fragmentation model, which are both supported by the observations of color coherence phenomena in e^+e^- annihilations.

The shower-based MC simulations were performed at the particle (hadron) level after the nonperturbative hadronization process, whereas the JETRAD predictions were at the parton level. Detector η and energy resolution effects were included in all predictions. The

generated events were subsequently processed using the same criteria employed for analyzing the data.

The β distributions, normalized to the total number of events, for the data and HERWIG and ISAJET predictions are shown in Fig. 3 for both central and forward regions. In each case the data peak near $\beta = \pi$ and this enhancement is more dramatic for higher η . The shape of these distributions is sensitive not only to the process dynamics but also to phase space effects resulting from our jet and event selection criteria. For both regions, HERWIG is in good agreement with the data, whereas ISAJET shows systematic deviations from the observed distributions.

The ratios of the observed β distributions relative to the MC predictions for both η regions are shown in Fig. 4. The data show a clear enhancement of events compared to ISAJET near the event plane (i.e., the plane defined by the directions of the second jet and the beam axis, $\beta = 0, \pi$) and a depletion in the transverse plane ($\beta = \frac{\pi}{2}$). This is consistent with the expectation from initial-to-final state color interference that the rate of soft jet emission around the event plane be enhanced with respect to the transverse plane. The PYTHIA predictions include string fragmentation. Without AO the PYTHIA distributions are significantly different from the data, while with AO turned on there is much better agreement, although there are still some residual differences in the “near beam” region. In addition, from the $\frac{\text{Data}}{\text{HERWIG}}$ and $\frac{\text{Data}}{\text{JETRAD}}$ β distributions, we conclude that both the AO approximation and $\mathcal{O}(\alpha_s^3)$ QCD describe the coherence effects seen in data in both η regions.

The main sources of uncertainty on the data β distributions are summarized in Table I. Since we report event normalized distributions, any possible uncertainty on quantities that affect the overall rate of events is minimized. For both η regions the statistical and systematic uncertainties are comparable. Sources of systematic uncertainty arise from the jet energy calibration, a possible η dependence of the jet reconstruction efficiency, and small η biases caused by the jet reconstruction algorithm.

We have also examined three main sources of systematic uncertainty related to the MC predictions. Varying the jet energy resolution within its measured uncertainties resulted in changes to the MC β distributions of less than 2.6% (2.8%) in the central (forward) region. The effect of using different parton distribution functions (CTEQ2ML, CTEQ2MF, and CTEQ2MS [19]) was examined with JETRAD and found to produce variations of less than 2.0% in the central and forward regions. The JETRAD β distributions varied by less than 1.3% (2.5%) in the central (forward) region when the renormalization and factorization scales varied from $E_{T1}/2$ to $2E_{T1}$.

Table II shows the χ^2 values of fits to the various $\frac{\text{Data}}{\text{MonteCarlo}}$ ratios with a constant for the central and forward regions as well as for the combined sample with $|\eta_2| < 1.5$. All uncorrelated systematic uncertainties (i.e., energy scale and η bias corrections) in the data were added in quadrature with the statistical uncertainties and were included in the calculation of χ^2 . The uncorrelated systematic uncertainty due to jet energy resolution was also added in quadrature with the statistical uncertainties of the MC predictions. From the χ^2 values we conclude that HERWIG and JETRAD agree best with our data for both η regions, whereas ISAJET clearly disagrees with the data. In addition, from the data to PYTHIA comparisons we conclude that for the process under study, string fragmentation alone cannot accommodate the effects seen in the data. The AO approximation is an element of parton-shower event generators that needs to be included if color coherence effects

are to be modeled successfully.

The data β distributions were also compared to the predictions of HERWIG at the parton level (before the nonperturbative hadronization stage). From the comparison of the $\frac{\text{Data}}{\text{HERWIG}}$ ratios at the parton and particle level we conclude that the hadronization effects as modeled by HERWIG are negligible and do not influence our results.

We processed a limited HERWIG event sample through a full GEANT based detector simulation [20] to investigate any possible detector effects not accounted for in the jet energy and η resolutions. From the comparison of the β distributions at the particle and detector levels such residual detector effects were found to be negligible.

We have presented a study of color coherent radiation in multijet events in $p\bar{p}$ collisions. We have measured the spatial correlations between the second and third leading E_T jets in the central and in forward pseudorapidity regions. Comparisons of the data distributions with various color coherence implementations demonstrate a strong presence of initial-to-final state interference. Parton shower MC simulations that implement color interference by means of angular ordering reproduce the data angular distributions well, with HERWIG giving the best representation. Striking differences are found between the data and MC models that do not incorporate color coherence effects in the parton shower development. Our results also indicate that coherence effects as predicted by a $2 \rightarrow 3$ partonic level calculation provide a good representation of our data, giving additional evidence supporting the validity of the local parton-hadron duality hypothesis.

We express our deep appreciation to V. Khoze and T. Sjöstrand for numerous valuable discussions on this work. We also thank T. Sjöstrand for helping us with the color coherence implementations in PYTHIA. We thank the staffs at Fermilab and collaborating institutions for their contributions to this work, and acknowledge support from the Department of Energy and National Science Foundation (U.S.A.), Commissariat à L'Énergie Atomique (France), State Committee for Science and Technology and Ministry for Atomic Energy (Russia), CNPq (Brazil), Departments of Atomic Energy and Science and Education (India), Colciencias (Colombia), CONACyT (Mexico), Ministry of Education and KOSEF (Korea), and CONICET and UBACyT (Argentina).

REFERENCES

* Visitor from Universidad San Francisco de Quito, Quito, Ecuador.

† Visitor from IHEP, Beijing, China.

- [1] JADE Collaboration, W. Bartel *et al.*, Phys. Lett. **B101**, 129 (1981); Zeit. Phys. **C21**, 37 (1983); Phys. Lett. **B134**, 275 (1984); Phys. Lett. **B157**, 340 (1985).
- [2] TPC/2 γ Collaboration, H. Aihara *et al.*, Phys. Rev. Lett. **54**, 270 (1985); Zeit. Phys. **C28**, 31 (1985); Phys. Rev. Lett. **57**, 945 (1986).
- [3] TASSO Collaboration, M. Althoff *et al.*, Zeit. Phys. **C29**, 29 (1985).
- [4] MARK2 Collaboration, P.D. Sheldon *et al.*, Phys. Rev. Lett. **57**, 1398 (1986).
- [5] OPAL Collaboration, M.Z. Akrawy *et al.*, Phys. Lett. **B247**, 617 (1990); Phys. Lett. **B261**, 334 (1991); P.D. Acton *et al.*, Phys. Lett. **B287**, 401 (1992); Zeit. Phys. **C58**, 207 (1993).
- [6] L3 Collaboration, M. Acciarri *et al.*, Phys. Lett. **B353**, 145 (1995).
- [7] B. Andersson, G. Gustafson, and T. Sjöstrand, Phys. Lett. **B94**, 211 (1980).
- [8] Ya.I. Azimov, Yu.L. Dokshitzer, V.A. Khoze, and S.I. Troyan, Phys. Lett. **B165**, 147 (1985); Sov. Journ. Nucl. Phys. **43**, 95 (1986).
- [9] R.K. Ellis, G. Marchesini, and B.R. Webber, Nucl. Phys. **B286**, 643 (1987); Erratum Nucl. Phys. **B294**, 1180 (1987).
- [10] Yu.L. Dokshitzer, V.A. Khoze, A.H. Mueller, and S.I. Troyan, Basics of Perturbative QCD, Editions Frontières (1991); Rev. Mod. Phys. **60**, 373 (1988); Yu.L. Dokshitzer, V.A. Khoze, and S.I. Troyan, Sov. Journ. Nucl. Phys. **46**, 712 (1987).
- [11] CDF Collaboration, F. Abe *et al.*, Phys. Rev. D **50**, 5562 (1994).
- [12] DØ Collaboration, S. Abachi *et al.*, Nucl. Instrum. Meth. **A338**, 185 (1994).
- [13] D. Cullen-Vidal, Ph.D. Dissertation, Brown University, (1997) (unpublished).
- [14] DØ Collaboration, R. Kehoe, in Proceedings of the VIth International Conference on Calorimetry in High Energy Physics, Laboratori Nazionali di Frascati, Frascati, Italy, (1996).
- [15] F.E. Paige and S.D. Protopopescu, BNL report No. 38034, 1986 (unpublished).
- [16] G. Marchesini *et al.*, Computer Physics Commun. **67**, 465 (1992).
- [17] T. Sjöstrand, Computer Physics Commun. **82**, 74 (1994).
- [18] W.T. Giele, E.W.N. Glover, and D.A. Kosower, Nucl. Phys. **B403**, 633 (1993); Phys. Rev. Lett. **73**, 2019 (1994).
- [19] CTEQ Collaboration, H.L. Lai *et al.*, Phys. Rev. D **51**, 4763 (1995).
- [20] R. Brun *et al.*, “GEANT 3.14” (unpublished), CERN, DD/EE/84-1.

TABLES

TABLE I. Major uncertainties in the data β distributions.

Source of uncertainty	$ \eta_2 < 0.7$	$0.7 < \eta_2 < 1.5$
Jet energy scale corrections	2.2%	3.4%
Jet η bias correction	1.2%	1.7%
Jet reconstruction efficiency		
Near beam	+1.5%	+5.0%
Far beam	-0.5%	-2.0%
Statistical error	3.2%	4.3%

TABLE II. χ^2 values for 8 degrees of freedom of fits to the various $\frac{\text{Data}}{\text{MonteCarlo}}$ ratios of β distributions with a constant for the central, forward, and combined samples. Statistical and uncorrelated systematic uncertainties were included.

Event Generator	χ^2		
	$ \eta_2 < 0.7$	$0.7 < \eta_2 < 1.5$	$ \eta_2 < 1.5$
ISAJET	48.0	24.9	74.4
HERWIG	5.1	7.7	7.2
JETRAD	7.9	7.9	7.2
PYTHIA			
String fragmentation, but no AO	77.2	62.9	126.0
String fragmentation, and AO	12.7	11.3	19.3

FIGURE CAPTIONS

Figure 1 Color flow diagrams for (a) $q\bar{q}$ and (b) qg scattering.

Figure 2 Three jet event topology illustrating the search disk (shaded area) for the softer third jet around the second jet.

Figure 3 Comparisons of the data β distributions to the predictions of ISAJET and HERWIG for (a), (b) central region and (c), (d) forward region. The error bars include statistical errors only.

Figure 4 Ratio of β distributions between data and the predictions of: (a) ISAJET, (b) PYTHIA with AO off, (c) PYTHIA with AO on, (d) HERWIG, (e) JETRAD for the central region; and (f)-(j) for the forward region respectively. The error bars include statistical and uncorrelated systematic uncertainties.

FIGURES

Figure 1

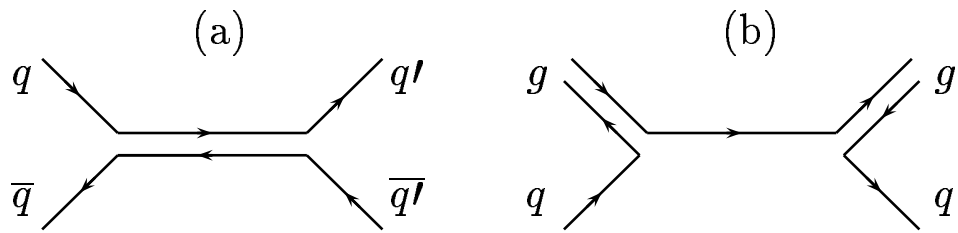


Figure 2

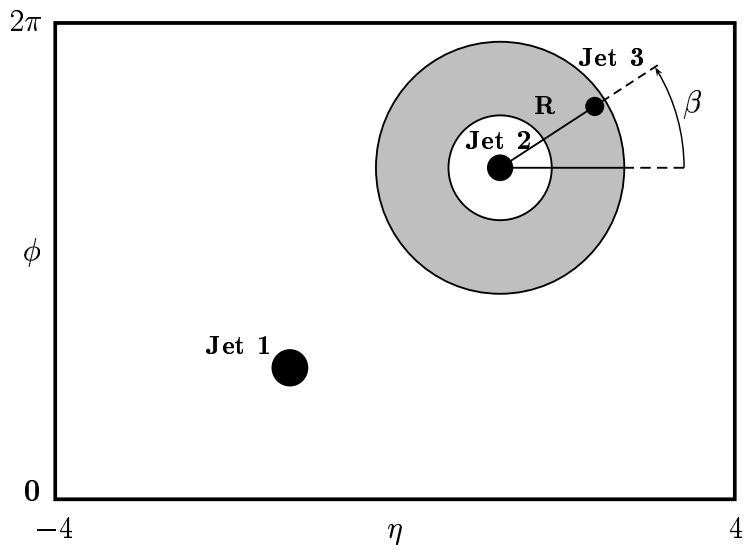


Figure 3

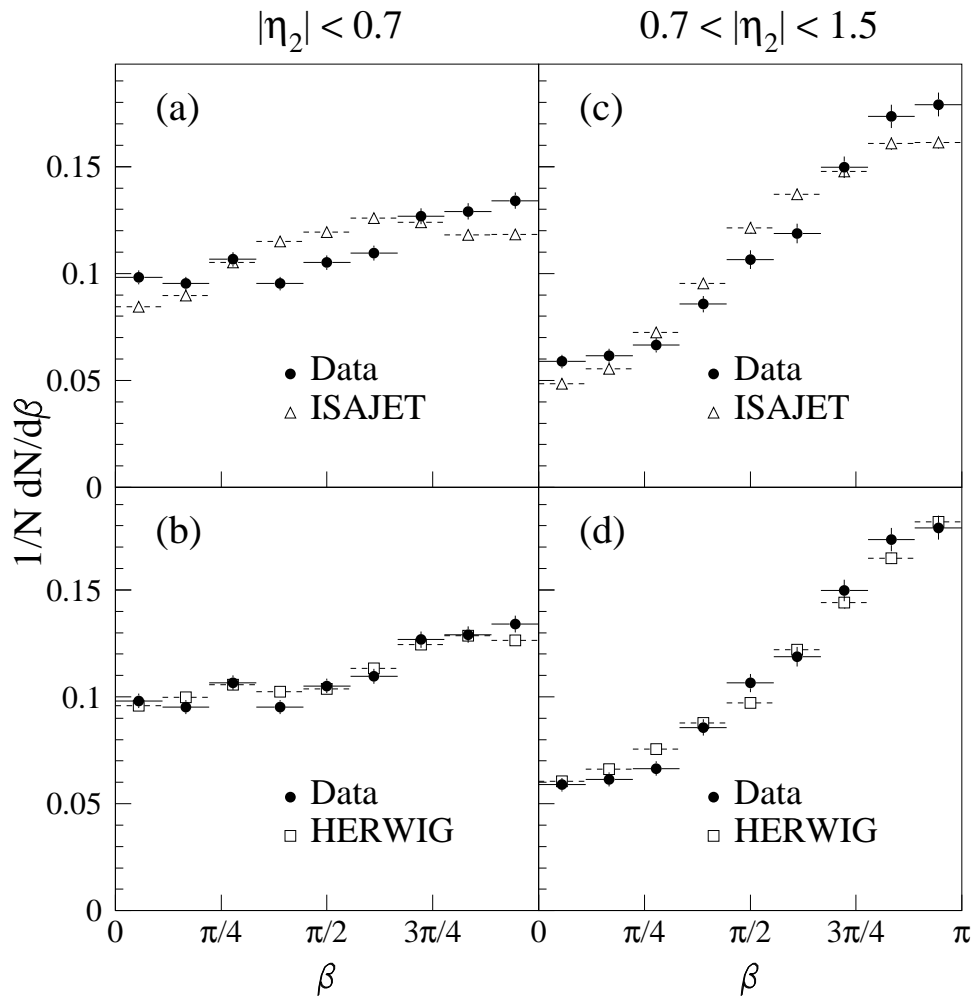


Figure 4

